Indian Journal of Chemical Technology
Vol. 28, May 2021, pp. 249-261

Optimization of process conditions to improve copper adsorption capacity of raw and treated Algerian bentonite: Characterization, kinetics and equilibrium study

Mohamed Ghrissi Bouaziz*, Leila Youcef*, Oussama Kheliel & Mohamed Charif Benalia

Research Laboratory in Subterranean and Surface Hydraulics, Civil Engineering and Hydraulic Department, University of Biskra,
PO Box 145, Biskra, 07000, Algeria
E-mail:ghrissimbouaziz@gmail.com, lyoucef2@yahoo.fr

Received 15 January 2021; accepted 7 April 2021

Raw bentonite (RB) locally available in Mostaganem (Algeria) deposit has been treated in the presence of NaOH (B-NaOH), $MgCl_2$ (B-$MgCl_2$) and H_2SO_4 (B-H_2SO_4) to improve its adsorption ability for the removal of copper ions from aqueous solutions. Characterization of all adsorbents supported montmorillonite, illite and kaolinite as major clay minerals identified for the raw and treated bentonites and proved the aluminosilicate structure of the clays. In synthetic solutions, the adsorption equilibrium of copper onto RB, B-$MgCl_2$ and B-H_2SO_4 is reached in 30 min. while, equilibrium is reached after 4 hours when using B-NaOH. The adsorption kinetics are well described by the pseudo-second-order model. The adsorption of copper is *p*H-dependent. The Langmuir, Freundlich and Dubinin-Radushkevich isotherms indicate a suitable fit between the experimental data and models. The corresponding parameters indicate that the sorption mechanism might be physical in nature. The maximum adsorption capacities of Langmuir that are obtained are in the following order 25.1 mg/g (RB) < 28.03 mg/g (B-H_2SO_4) < 39.89 mg/g (B-$MgCl_2$) < 72.80 mg/g (B-NaOH). The removal efficiency of copper in industrial wastewater was 45.75 %, 55.22 %, 63.27 % and 70.39 % using RB, B-$MgCl_2$, B-H_2SO_4 and B-NaOH, respectively. The B-NaOH exhibit a higher adsorption capacity of copper with the other tested bentonites.

Keywords: Treated bentonite, Characterization, Copper, Adsorption, Kinetic, Equilibrium.

Heavy metals are commonly used in various industrial processes such as mining, metal cleaning, plating baths, painting, paperboard mills, electroplating, fertilizer industries and ceramics, in the textile and photographic industries, pharmaceuticals that are the potential sources of Cu(II) ions in industrial effluents[1-3]. These pollutants have particular chemical properties that give them, at a rate above the standards, a toxicity for humans and living organisms of the animal and plant reign[1].

Among these substances, copper is considered an essential element of life for living organisms. Consumed at concentrations exceeding the pot ability standard, 2 mg/L of copper[4], it is considered toxic. In the body, copper has been associated with many health problems such as kidney damage, high fever, hemolysis and vomiting…etc[1].

Different methods of treating effluents and contaminated water containing metal pollutants like Cu(II) ions have been developed over the years to prevent their deleterious impact on public health and the ecosystem. Treatment include such as chemical precipitation[5-7], electrocoagulation[8], coagulation flocculation, cation-exchange and membrane separation[9-12]. However, some of these techniques have some disadvantages such as complicated treatment processes, production of toxic by-products, high-energy consumption and cost.

Adsorption has recently become one of the alternative treatment methods for wastewater contaminated with heavy metals. The adsorption mass transfer is a process in which a contaminant passes from the liquid phase to the surface of the solid phase and relates to the physical and/or chemical interactions. Technical applicability and cost-effectiveness are key factors that play a decisive role in the selection of the most suitable adsorbent for purifying of inorganic pollutants from contaminated wastewater[13]. Adsorption is an effective separation process due to its low operating cost and low energy consumption[14].

Natural clays, such as bentonite, have been used to challenge chemical pollutants from wastewater. In addition, bentonite has a net negative surface charge that renders effective removal of cationic compounds from water[15,16]. The expanding layer of aluminosilicates with different surface exchangeable cations such as calcium, sodium, magnesium, and potassium provides the affinity and capacity for bentonite adsorption. Bentonite adsorption is a refered method in water and wastewater treatment owing to its simple process, cheap, and abundance supply of adsorbent, and excellent adsorbent properties rendering exceptional removal efficiencies toward target pollutants[16].

The results involving the removal of copper with natural bentonite clay acid-activated[17], hydroxyl activated[14] and salt activated[18] are significant and promising. All of these studies have applied the sorptive removal process due to its efficiency and low cost.

In Algeria, existing literature confirmed the wide application of Algerian natural and treated bentonite for copper removal from aqueous solutions[19-27]. Although the results involving the removal of copper with Algerian bentonites are relevant and impressive, there is still a need to optimize process conditions for the treated wastewater and to improve the adsorption capacity of bentonites which is submitted for structural modification. The promising results obtained related to be above drive us to continue the work on this topic to evaluate other potential perspectivs.

Thus, in the present work, we report the use of Raw Bentonite (RB) obtained from the deposit of Mostaganem (Algeria). This bentonite was treated individually in presence of H_2SO_4, NaOH and $MgCl_2$ to improve its adsorption ability for the removal of copper ions from aqueous solutions. Initially, a systematic characterization of the RB and treated bentonites was carried out. The clays were characterized using X-Ray Diffraction (XRD), Attenuated Total Reflectance Fourier Transform Infrared Spectroscopy (ATR-FTIR), Scanning Electron Microscopy (SEM) and the point of zero charge (pHpzc) to evaluate structural modifications. Using synthetic solutions of distilled water, the effect of many reactional parameters such as contact time, pH of solutions, the dosage of the adsorbent, initial concentration of metal were investigated. To understand the adsorption mechanism, kinetic models as pseudo-first-order PFO), pseudo-second-order (PSO) and intra-particle diffusion were applied to experimental data. In order to describe the sorption equilibrium, Langmuir, Freundlich and Dubinin-Radushkevich isotherms were tested. The raw and treated bentonites were tested for their potential use in removal of Cu(II) ions from the industrial wastewater. The discussion of findings aim to approach the research gaps with new considerations based on the obtained experimental data and to provide insight into to the performance of Algerian modified bentonite in adsorption of copper in wastewater.

Experimental Section

Adsorbents

Raw bentonite

The local bentonite used namely raw bentonite (RB) was supplied by ENOF (Algerian bentonite Company-National Enterprise for Non-Ferrous Mining Products and of Useful Substances). This naturally abundant clay is locally available in the M'Zila deposit in Mostaganem (Algeria) was used in its raw state. Some characteristics of this clay were determined by the laboratory of the ENOF. The specific surface analysis of the RB was found to be 19.81 m^2/g. The major cation in this bentonite is calcium with a capacity of exchange that of 46.7 meq/100g that is the highest compared to other mineral elements[28]. Bentonite obtained was sieved to obtain particles size less than < 2 μm, it was dried at 75°C and then grounded.

Bentonite treatments

- The treated bentonite with NaOH was obtained by mixing 50 g of the RB with NaOH solution (1 N) at a weight ratio of 20% into a reactor of 250 mL[14]. Under continuous stirring, the mixture was heated to about 100°C for 1 hour. The treated bentonite was then filtered and washed with distilled water until the pH of the filtrate was between 6 and 7. Finally, the clay was dried at 110 °C and named B-NaOH.
- The treated bentonite with $MgCl_2$ was obtained by introducing 50 g of the RB into 500 mL of a 1 M solution of $MgCl_2$, $6H_2O$ and stirred for 24 hours. The filtered mixture was washed with distilled water until the chloride ions disappear. The clay was then dried at 110°C[29] and designated B-$MgCl_2$.
- The treated bentonite with H_2SO_4 was obtained by the introduction of 50 g of RB into a 250 mL reactor, followed by the sulfuric acid solution (10% H_2SO_4) in a mass ratio of 20%[14]. The mixture was then heated to about 100°C for 1 hour. The activated bentonite was then, filtered and washed with distilled water. When all traces

of the acid disappears and no longer gives the reaction of the sulfates with the barium chloride, the bentonite was dried at 110°C for 1 hour. The clay was named B-H_2SO_4.

Characterization of adsorbents

The structure of adsorbents was characterized by powder X-ray diffraction (XRD) using Benchtop X-ray diffractometer for phase analysis (Miniflex 600) over a range of 2θ between 2°- 70° and scanning rate of 0.03° min^{-1}. The surface functional groups of the bentonites were studied by ATR-FTIR spectroscopy using Perkin-Elmer Spectrum Two. ATR-FTIR spectrum was recorded in wavenumber range of 400-4000 cm^{-1}. The Scanning Electron Microscopy (SEM) in conjunction with EDX (Energy dispersive x-ray spectroscopy) of bentonite samples were obtained by using a scanning electron microscope (Tescan VGA3). This analysis is used to study the surface morphology and chemical composition of clay samples. The point of zero charge (pH_{PZC}) was measured according to the method described by Sepulveda and Santana[30] and Chang *et al.*[31]. For the determination pH_{PZC} of adsorbents, 0.1 M NaCl solution was used.

Batch adsorption experiments

Analytical grade Cu(II) sulfate pentahydrate ($CuSO_4$, 5 H_2O) (Sigma-Aldrich) was used for preparation of the synthetic solutions in distilled water.

The tests were carried out using magnetic stirrirer by contacting the sample (50 mL) with a well-determined dose of the adsorbent. The solid /liquid separation of the taken sample was carried out by filtration under a vacuum using a membrane of 0.45 µm porosity. Thereaction parameters were varied including the influence of stirring time (0 to 6 hours), the pH of solution (from 2 to 10), the effect of the dose of bentonite (from 0.1 to 4 g/L) and the initial content of metal ions (from 1 to 100 mg/L). The *p*H of water samples was measured using a HANNA *p*H meter model *p*H 210. All tests of adsorption in synthetic solutions were performed at *p*H = 5.5 (except for the *p*H influence study). HCl (0.1 M) or NaOH (0.1 M) were used to adjust the *p*H of the solutions.

Using the Industrial wastewater of a cable industry company (ENICAB) located in Biskra (Algeria), the influence of stirring time (0 to 6 hours) was tested.Physico-chemical parameters of Industrial wastewater were determined by standard methods of analysis[32] or by the methods described in the user guides of the equipment.

The residual Cu(II) content was measured by atomic absorption spectrophotometer (Schimadzu AA 6200). The amounts of copper adsorbed onto clays at any time (q_t (mg/g)), at equilibrium (q_e (mg/g)), and the percentage removal (%) of copper, were calculated based on the Equation (1), Equation (2) and Equation (3):

$$q_t = \frac{(Co - Ct)}{m} V \quad \ldots (1)$$

$$q_e = \frac{(Co - Ce)}{m} V \quad \ldots (2)$$

$$\text{Copper removal (\%)} = \frac{(C_0 - C_e)}{C_0} 100 \quad \ldots (3)$$

Where C_0 (mg/L), C_t (mg/L) and Ce (mg/L) are the initial concentration, concentration at time t and equilibrium concentrations of copper, V (L) is the volume of metal solution and m (g) is the mass of the used adsorbent.

Results and Discussion

Results of characterization of adsorbents

X-ray diffraction analysis

The X-ray diffraction patterns of samples are shown in Fig. 1(a). X-ray diffractogram of the raw bentonite (RB) showed a characteristic peak at 2θ = 7.07° (d= 12.50 A°). Such a pattern is characteristic of smectite montmorillonite and is in good agreement with earlier works[20,22,33]. Other peaks corresponding to the illite and Kaolinite appeared at 2θ = 8.78° (d= 10.06 A°) and 2θ = 12.37° (d= 7.15A°) respectively. This means that Montmorillonite, Illite and Kaolinite as major clay minerals that were identified in the tested RB. In addition, RB contains impurities that are characterized by a strong reflection at 2θ = 26.68° identified as quartz, calcite with peaks at 2θ = 29.44° and 47.55°, respectively and feldspar with reflection at 2θ = 30.74°. Associated montmorillonite, illite, kaolinite and quartz impurities were also found in all adsorbent. The feldspar and calcite (at 2θ = 47.55°) considered as impurities in the raw material clay disappears in the acid-activated sample (B-H_2SO_4) and the bentonite treated in presence of $MgCl_2$ (B-$MgCl_2$).The treatment of bentonite with NaOH and $MgCl_2$ increased the characteristic d_{001} peak values of montmorillonite to 14.45 A° and 14.86 A°, respectively and the acid treatment with H_2SO_4 reduced it to 10.04 A°. However, the peak was much less intense compared to the raw bentonite. This phenomenon is accompanied by the displacement of its position from 7.07A° to 6.12A° , 5.94A ° and 8.80 A°, respectively which confirms that the RB has been changed after treatment. This is in agreement with previous results cited[19,20,22,24,26,33]. The increase in the interlayer distance d_{001} can be attributed to the intercalation of the inorganic ligand, which is preferentially oriented parallel to the plane of the layer[33]. It is known also that the process of acid treatment leaches out impurities such as calcite and some ions such as Mg^{2+}, Ca^{2+} and Al^{3+} (Ref. 20).

Attenuated Total Reflectance Fourier Transform Infrared Spectroscopy analysis

The Attenuated Total Reflectance Fourier Transform Infrared spectra (ATR-FTIR) of RB and activated bentonites are presented in Fig. 1(b). All the detected function proved the aluminosilicate structure of the clay. The presence of water molecules was due to the adsorption related to the swelling propriety of the material. The band observed at 3620 cm^{-1} is characteristic of aluminous smectites[34]. The peak at 3620 cm^{-1} could be attributed to the -OH stretching vibration of the Al-OH groups and the -OH stretching vibration of bound water, respectively[31]. Similarly with the band at 915 cm^{-1} of deformation[35]. Weak (less intense) band noticed at 3697 cm^{-1} is attributed

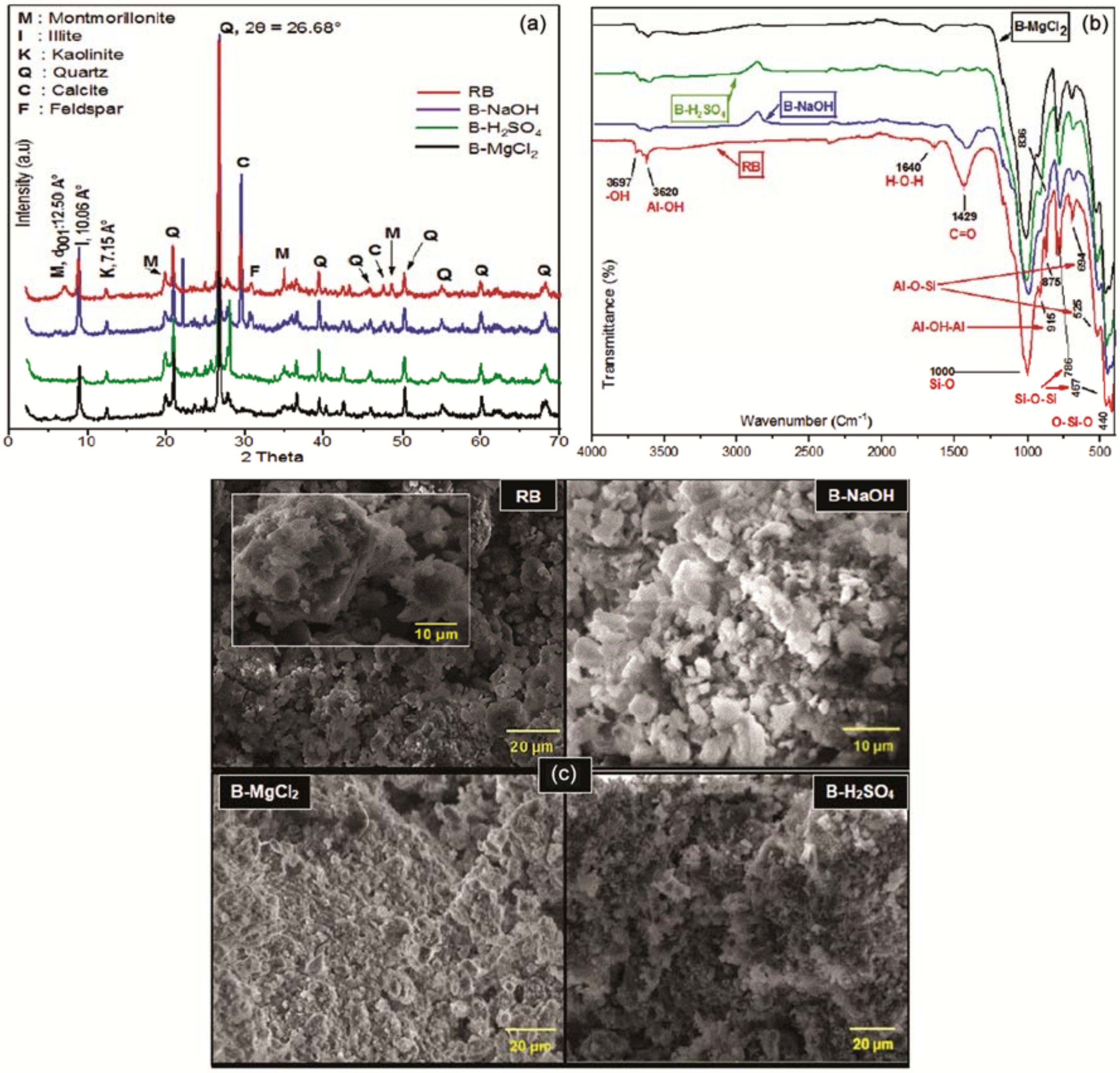

Fig. 1— (a) XRD patterns, (b) Attenuated Total Reflectance Fourier Transform Infrared spectra(ATR-FTIR) and (c) Scanning electron microscopy (SEM) micrographs of raw and treated bentonites.

to the valence vibrations of the hydroxyl (-OH) bond in the lamellar space[36,37] of the raw and treated bentonites. In addition, for all four clays, the band at 1640 cm^{-1} can be attributed to both OH stretching vibration and $\delta(H_2O)$ deformation[19,33].

A large band that appeared at 1000 cm^{-1}, is corresponding to the Si-O vibration of the bentonite tetrahedral layer[38,39,24]. Three bending vibrations of hydroxyl groups associated with Al^{3+} at 915 cm^{-1} (Al-OH-Al), Fe $^{3+}$ at 875 cm^{-1} (Al-Fe-OH) and Mg^{2+} at 836 cm^{-1} (Al-Mg-OH) confirm the substitution in the octahedral layer[36]. The rest of the bands between 1000 and 525 cm^{-1} in all samples are due to stretching vibrations of Si-O, Si-O-Si, OH attached to Al^{3+}, Fe^{3+} and Mg^{2+} groups and the silica quartz impurities, respectively[19,31,40]. The characteristic vibration peaks of montmorillonite are at 467.5 cm^{-1} (Si–O–Si) bending[22]. The main change of spectra that are found after treatment with H_2SO_4 and $MgCl_2$ is the disappearance of the absorption band centered at 1429 cm^{-1}indicates the release of carbonate anions (CO_3^{-2}). This is due to the dissolution of calcite ($CaCO_3$)[41]. These confirmed the absence of calcite, as shown in the XRD patterns.

Scanning Electron Microscopy (SEM) analysis

SEM micrographs of clays tested (Fig.1(c)) showed a crystalline structure with multiple voids and micropores of pseudo-spherical smectite aggregates. Some other agglomerated unshaped fragments can also be seen. This smooth presents a high porosity of the bentonite particles that confers it the character of being a good adsorbent.

EDX analysis (Table 1) confirms that the predominant cation in the RB is calcium and the clay is an aluminosilicate. The magnesium content increases after pillaring from 2.53% to 3.03% in $B\text{-}MgCl_2$, which could confirm the intercalation of magnesium ions in the bentonite network. This is associated with a significant decrease in the content of calcium from 6.73% to 0.43%. Similarly, for B-NaOH, the sodium content increases after treatment with NaOH from 0.82% to 1.44%. In the case of $B\text{-}H_2SO_4$, the decrease in the content of calcium (from 6.73% to 2.03%) and magnesium (2.53% to 0.93%) confirms that the process of acid treatment leaches out some ions such as Mg^{2+} and Ca^{2+}.

Table 1 — EDX analysis of raw and treated bentonites (Composition (Wt %)).

Element	RB	B-NaOH	$B\text{-}H_2SO_4$	$B\text{-}MgCl_2$
O	52.55	52.71	53.17	49.45
Si	21.51	24.66	29.88	32.36
Al	8.55	7.47	8.58	8.83
Ca	6.73	6.29	2.03	0.43
Mg	2.53	1.65	0.93	3.03
Na	0.82	1.44	0.4	0.33
K	2.46	1.04	1.31	2.22
Fe	4.55	4.74	4.36	3.35

Results of adsorption experiments

Kinetics study

For an initial concentration of metal around 10 mg/L and in contact of 1 g/L of the adsorbent, and as a function of contact time, the results obtained (Fig. 2(a)) show that at the equilibrium, the adsorption equilibrium of copper onto RB, $B\text{-}MgCl_2$ and $B\text{-}H_2SO_4$ clays was reached in 30 min. While, equilibrium was reached after 4 hours when using B-NaOH. The removal efficiency of copper was

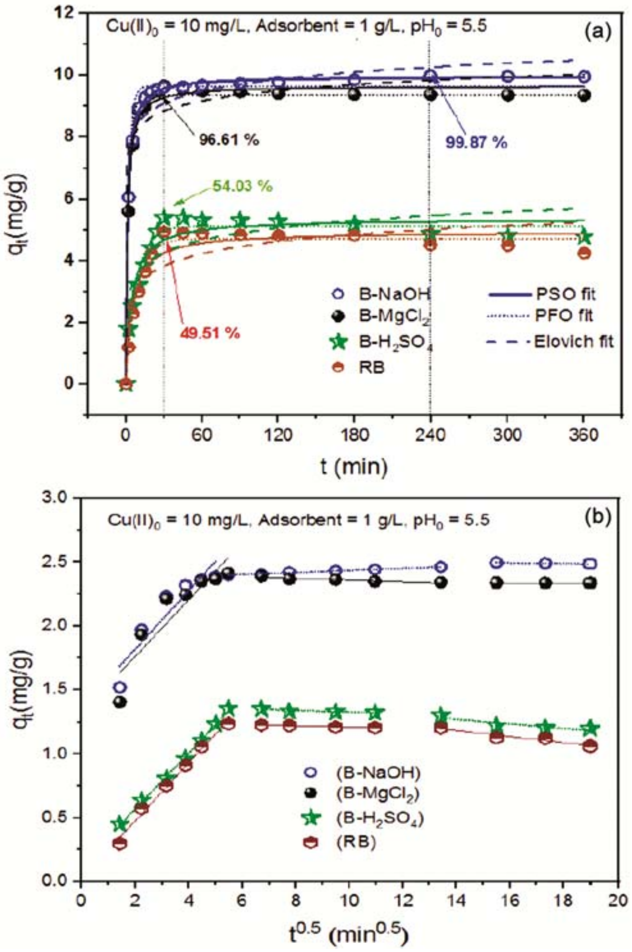

Fig. 2 —(a) Effect of contact time on the Cu(II) adsorption onto raw and treated bentonites and plots of kinetic models (Pseudo-first-order (PFO), Pseudo-second-order (PSO) and Elovich, (b) Intraparticle diffusion model.

49.51 %, 54.03 %, 96.61 % and 99.87 % using RB, B-H_2SO_4, B-$MgCl_2$, and B-NaOH respectively.

For models were used to interpret the experimental data obtained during the tests of the kinetic adsorption of Cu(II) ions onto the bentonites. The kinetic data was simulated by using nonlinear isotherm of Pseudo-first-order (PFO)[42], Pseudo-second-order (PSO)[43] and Elovich[44]. The linear model of intraparticle diffusion[45] was also tested. The forms of those models were expressed in equations Equation (4) to Equation (7), respectively.

$$PFO\,model{:}\ q_t = q_e\left(1-e^{-k_1 t}\right) \quad \ldots (4)$$

$$PSO\ model{:}\ q_t = \frac{q_e^2 k_2 t}{1+q_e k_2 t} \quad \ldots (5)$$

$$Elovich\ model{:}\ q_t = \frac{1}{\beta} \times \ln(1\times\alpha\times\beta\times t) \quad \ldots (6)$$

$$Intraparticle\ diffusion\ model{:}\ q_t = k_{int}t^{1/2}+C \quad \ldots (7)$$

Where q_e (mg/g) and q_t (mg/g) are the amount of copper adsorbed at equilibrium and at time t (min) respectively. k_1 (min^{-1}) is the rate constant for the pseudo-first-order and k_2 (g/min.mg) is the rate constant for pseudo-second-order. α (mg/g/min) is the initial sorption rate and β (mg g^{-1}) is the desorption constant related to the extent of surface coverage and activation energy for chemisorption. k_{int} (mg/g $min^{1/2}$) is the intraparticle diffusion rate constant and C (mg/g) is constant related to the thickness of the boundary layer.

The best fitting sorption kinetic nonlinear models (PFO, PSO and Elovich) were validated using two different statistical error functions namely coefficient of determination (R^2)[46] and Chi-square (χ^2)[47].The following expressions (Equation (8) and Equation(9))are used to determine R^2 and χ^2:

$$R^2=1-\frac{\Sigma\left(q_{e,\,exp}-q_{e,\,cal}\right)^2}{\Sigma\left(q_{e,\,exp}-q_{e,\,mean}\right)^2} \quad \ldots (8)$$

$$\chi^2 = \sum_{i=1}^{n}\frac{(qe,\,exp-qe,cal)^2}{qe,\,cal} \quad \ldots (9)$$

Where $q_{e,\,exp}$ is the equilibrium adsorption capacity found from the experiment, $q_{e,cal}$ is the prediction from the model for corresponding to Ce,$q_{e,\,mean}$ is the mean of the $q_{e,exp}$ values and n is the number of experiments.

To estimate the goodness-of-fit of the models to the experimental data, the coefficient of determination is such that R^2 is close to 1 and χ^2 is close to zero. A high χ^2 value indicates a large difference between the experimental and the calculated model values.

For linear model of interaparticle diffusion, the Residual Sum of Squares (RSS) was also determined. RSS function is a statistical tool used by several researchers to judge the agreement between the experimental quantity of the pollutant adsorbed and the calculated quantity adsorbed[48]. Lower is the value, the curve is more adequate to the experimental values. It is expressed by the following equation (Equation (10)):

$$RSS = \sum_{i=1}^{n}(q_{e,exp}-q_{e,calc})^2 \quad \ldots (10)$$

The experimental data of time-dependence adsorption of Cu(II) on each tested bentonites were described by kinetic models (PFO, PSO and Elovich) (Fig. 2(a)). The corresponding kinetic parameters from the PFO, PSO and Elovich models are summarized in Table 2 which shows that all of the studied adsorption systems could be better described by the nonlinear PSO model over the entire range of contact time with higher value of correlation coefficient (R^2> 0.90) as compared with other models. Other than the correlation coefficients, evaluation of the suitability of the kinetic models also arises from the comparison between the calculated ($q_{e,\,cal}$) and the experimentally determined ($q_{e,\,exp}$). From Table 2, it can be noticed that the q_e calculated by the PSO model was closer and comparable to the experimental determined values ($q_{e,\,exp}$). In addition, there was good statistical signification (χ^2value ≈ 0, R^2 ≈ 1). Therefore, it can be concluded that the PSO equation is the suitable kinetic model that describes the kinetic adsorption of Cu(II) ions on the bentonites tested. This is in agreement with the study that was carried out on the adsorption of divalent ions by raw and treated bentonites[27, 31].

As shown in Fig.2 (b), the intraparticle diffusion plots are linear, and no straight lines pass through the origin. This result indicates that the pore diffusions were not the only step controlling the adsorptions of copper onto bentonite[31,33]. It can be also seen from Fig. 2(b) that three steps governed the copper

Table 2 — Kinetic parameters ofPFO, PSO, Elovich and intraparticle diffusion models for adsorption of Cu(II) ions in synthetic solutions on raw and treated bentonites.

Model	Parameter	B-NaOH	B-MgCl$_2$	B-H$_2$SO$_4$	RB
Pseudo First Order	$q_{e,exp}$(mg/g)	9.987	9.661	5.403	4.951
	$q_{e,cal}$(mg/g)	9.638	9.364	5.130	4.718
	k1 (1/min)	0.428	0.401	0.118	0.116
	R^2	0.984	0.992	0.958	0.976
	χ2	0.11	0.053	0.11	0.06
Pseudo Second Order	$q_{e,cal}$(mg/g)	9.968	9.658	5.372	4.950
	k2 (g/mg.min)	0.079	0.082	0.041	0.041
	R^2	0.999	0.991	0.941	0.946
	χ2	0.005	0.06	0.153	0.134
Elovich	β (mg/g)	1.778	2.070	1.746	1.753
	α (mg/g.min)	194713.292	$1.392\text{x}10^6$	33.414	15.869
	R^2	0.953	0.916	0.816	0.807
	χ2	0.321	0.546	0.481	0.482
Intraparticle Diffusion	*1st Stage*				
	$K_{int,\,1}$ (mg/mg.min$^{1/2}$)	0.229	0.224	0.219	0.227
	C_1 (mg/g)	1.362	1.318	0.133	0.022
	R^2	0.861	0.836	0.998	0.991
	RSS	0.079	0.128	0.001	0.005
	2nd Stage				
	$K_{int,\,2}$ (mg/mg.min$^{1/2}$)	0.008	0.007	0.006	-0.005
	C_2 (mg/g)	2.365	2.427	1.381	1.262
	R^2	0.989	0.866	0.846	0.973
	RSS	$2.841\text{x}10^{-5}$	$1.927\text{x}10^{-4}$	$5.861\text{x}10^{-5}$	$7.344\text{x}10^{-6}$
	3rd Stage				
	$K_{int,\,3}$ (mg/mg.min$^{1/2}$)	0.003	-7.275	0.018	-0.023
	C_3 (mg/g)	2.537	2.351	1.517	1.515
	R^2	0.974	0.832	0.838	0.925
	RSS	$1.08\text{x}10^{-6}$	$6.489\text{x}10^{-7}$	0.001	$7.667\text{x}10^{-4}$

adsorptions onto raw and treated bentonites. According to Table 2, for each tested bentonite, the values of intraparticle rate constants follow the order:$k_{int,1}>k_{int,\,2}>k_{int,\,3}$. The first linear portions had the steepest slopes, which suggest the instantaneous diffusion of copper ions from the solution to the external surfaces of the adsorbents and then rapid retention of Cu(II) ions on the exterior surfaces at the beginning of adsorption ($k_{int,1}$). As time went on adsorption of copper, the second linear parts of plots had lower slopes. The last linear portions indicated the equilibrium period during which the rates of intraparticle diffusion of Cu(II) ($k_{int,3}$) decreased significantly and the equilibrium was gradually attained. Comparing between the intraparticle diffusion results obtained for both adsorbents, it can be seen that the $k_{int,1}$ of the first diffusion step increased with the order of magnitude of the efficiency of the tested adsorbents (Table 2) as follows: $k_{int,1}$: B-NaOH> B-MgCl$_2$> B-H$_2$SO$_4$> RB. This means larger the intercept, the greater is the contribution of the surface sorption in the rate controlling step.

Effect of initial pH

The effects of initial *p*H of the solution (ranging from 2 to 10) on copper adsorption onto RB and treated bentonites were investigated. Fig. 3(a) shows that the uptake of copper ions by all bentonites was significantly influenced by the initial *p*H of solution. The sorption of copper relatively increased with increasing *p*H from 2 to 7. From *p*H 7 to 10, a plateau was observed with negligible differences in the copper uptake by both raw and treated bentonites.

The sorption behaviours of all adsorbents can be critically linked to their *p*H point of zero charge (pHpzc). Fig. 3(b) shows the plots for pHpzc determination for raw and treated bentonites. The pHpzc for the tested bentonites were determined as 7.52 to 9.68 (Fig. 3(b)). *p*Hzch is important for amphoteric clay such as bentonite because it demonstrates the properties of variable-charge surfaces at different *p*H[31]. If the *p*H of the solution is lower than the pHpzc, the edge sites of bentonite structure have positive charge developed arising from the protonation of variable-charged surface (OH groups) even though the basal sites possess negative charge density. Hence, electrostatic repulsion between the positively charged sorption sites and metal cations restricted the attachment of cations on adsorbent surfaces. On the contrary, when the *p*H of the solution exceeds pHpzc, the net charge on surfaces of adsorbents becomes negative due to the deprotonation of surface OH groups and the negative charges increase with solution *p*H. Surfaces with net negative charges attracts copper ions in the solutions through electrostatic action[3,31,49]. On the other hand, silica and alumina functional groups may be protonated as the solution *p*H lies below pHpzc.The hydrolysis of Si–OH or Al–OH bonds along the clay lattices produce different surface charges, as depicted by the following schemes ((1) and (2)) described by Putra *et al.*[50] and Alexander *et al.*[16]:

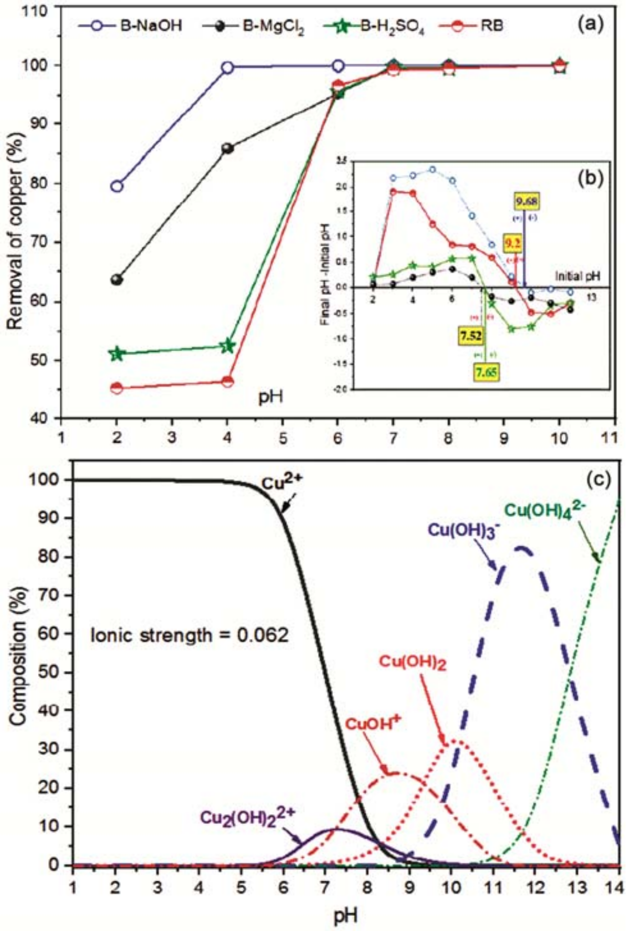

Fig. 3 — (a) Effect of pH on copper adsorption onto bentonites($Cu(II)_0$ = 10 mg/L, adsorbent dose = 1 g/L), (b) Point of zero charge for used adsorbents and (c) Copper dominant species according to *p*H variation in aqueous solution at 25°C using Visual MINTEQ Software (Version 3.0) ($Cu(II)_0$ = 10 mg/L).

pH<pHpzc :

$$\equiv AlOH + H^+ \rightarrow AlOH_2^+ \equiv Si\text{-}OH + H^+ Si\text{-}OH_2^+ \qquad \ldots (1)$$

pH>pHpzc :

$$\equiv AlOH + OH^- \rightarrow AlO^- + H_2O \equiv Si\text{-}OH + OH^- Si\text{-}O^- + H_2O \qquad \ldots (2)$$

In addition to the nature of the adsorbents, another property to be considered is the metal speciation at different *p*H[51,52]. The solution speciation of Cu (II) ions was modeled using the Visual MINTEQ software (Version 3.0)[53,54] at 25°C according to thepH variation of the solution (Fig. 3 (c)). It seems that the adsorption at higher pH values (> 7) involved the formation of the metal complexes ($Cu_2(OH)_2^{2+}$, $CuOH^+$ and $Cu(OH)_3^-$) as well as hydroxide precipitation ($Cu(OH)_2$).

Effect of adsorbent dosage

The effect of adsorbent dosage on removal of Cu(II) ions was investigated at different bentonite dosages and the results are plotted in Fig. 4. The percentage of the Cu(II) ions adsorption steeply increased with the adsorbent loading up from 0.1 g /L to 4 g/L (Fig. 4 (a)). This result can be explained by the fact that when the adsorbent ratio is small, the active sites for binding copper ions on the surface of bentonites metal ions on the surface of bentonites is less, so the adsorption efficiency is low. As the adsorbent dose increased, more active sites bind to metal ions, thus resulting in an increase in the adsorption efficiency until saturation[3,23,31].

As seen from Fig. 4(b), the amount of copper ions adsorbed per unit mass of adsorbent decreased with increasing adsorbent dosages. Other researchers[31,55,56] have defined a similar trend in bentonite dosage for metal ion adsorption. A possible reason is that in a system with high adsorbent content, the available metal ion concentrations are insufficient to saturate completely binding sites on the adsorbent, thus resulting in low adsorption capacity[31,57].

Effect ofthe initial concentration of copper

The effect of initial copper concentration on the adsorption process was investigated by varying initial Cu(II) ions concentration from 1 to 100 mg/L in the presence of 1 g/L of adsorbent. Results (Fig. 5) indicated that the removal of copper (%) in raw or treated bentonites decreased gradually with an increase in the initial concentration of Cu(II)ions. At low concentrations, the metal ions had a large number of available adsorption sites. However, at the higher initial metal concentrations, the competition of copper ions for adsorption sites of the adsorbent becomes important. As a result, each unit mass of adsorbent is subjected to higher amounts of Cu(II) ions. The adsorption sites became saturated, and no more sites were available for further sorption. Therefore, the adsorption of copper on bentonite is dependent on the initial metal concentration[23,24,27,31].

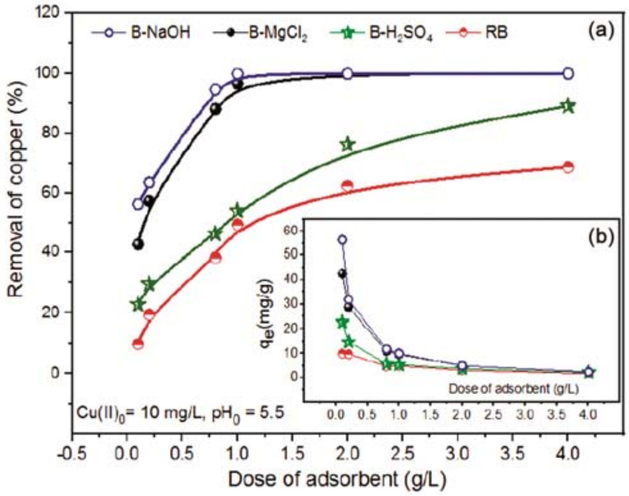

Fig. 4 — (a) Effect of bentonite dose on removal efficiency and (b) adsorption capacity of Cu(II) on tested adsorbent (pH_0 = 5.5, $Cu(II)_0$ = 10 mg/L, adsorbent dose = 0.1 g/L to 4 g/L).

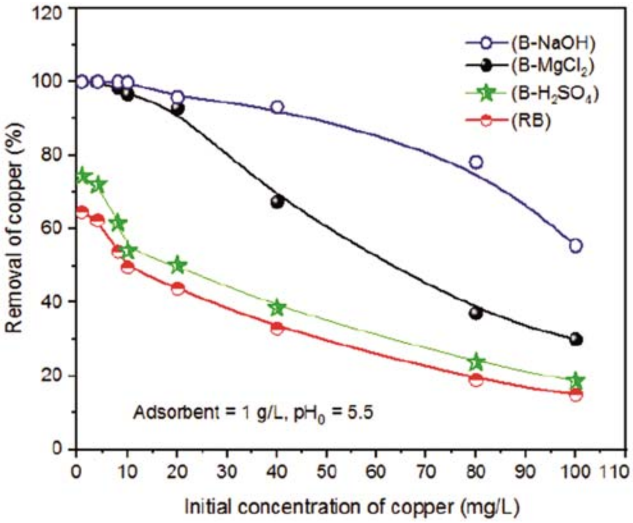

Fig.5 — Effect of initial metal concentration on adsorption efficiency onto raw and treated bentonites (pH_0 = 5.5, $Cu(II)_0$= 1-100 mg/L, adsorbent dose = 1 g/L).

Adsorption isotherms

The adsorption isotherm was studied to describe the distribution of Cu(II) ions at the adsorbent-liquid interface. The isotherm data were simulated by using nonlinear isotherms of Langmuir[58], Freundlich[59] and Dubinin-Radushkevich[60] isotherm to identify the appropriate model representing the sorption process (Fig. 6). The nonlinear forms of the Langmuir, Freundlich and Dubinin-Radushkevich are expressed in Equation (11), Equation(12) and Equation(13), respectively.

Langmuir model: $$q_e=\frac{Q^0_{max}K_LC_e}{1+K_LC_e} \qquad \dots (11)$$

Where q_e (mg/g) is the amount of copper adsorbed at equilibrium, Ce (mg/L) is the concentration of metal solution at equilibrium, Q^0_{max} (mg/g) is the maximum saturated monolayer adsorption capacity of the adsorbent, k_L (L/mg) is Langmuir constant related to the affinity between the adsorbent and adsorbate.

Freundlich model: $$q_e = K_F C_e^n \qquad \dots (12)$$

Where: K_F ((mg/g)/(mg/L)^n) is the Freundlich constant and n is dimensionless Freundlich intensity parameter (0<n<1).

Dubinin-Radushkevich model: $$q_e = q_{DR} e^{-K_{DR}\varepsilon^2} \qquad \dots (13)$$

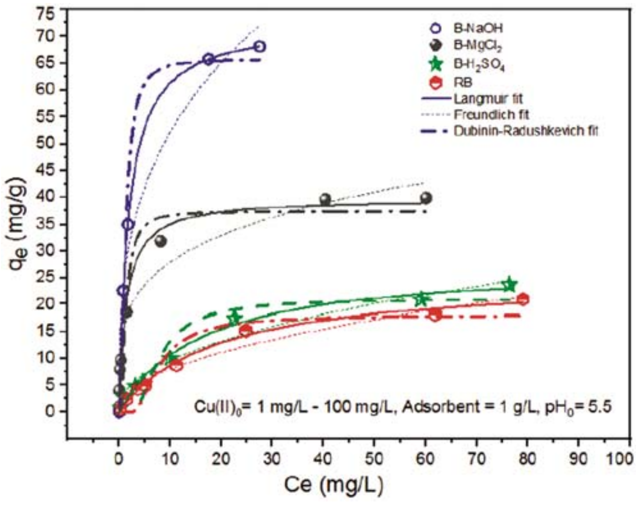

Fig.6 — Adsorption isotherms of copper onto raw and treated bentonites.

Where $\varepsilon = RT\ln(1+\frac{1}{Ce})$ and $E = \frac{1}{\sqrt{2K_{DR}}}$.

In this equation, q_{DR} (mg/g) is maximum sorption capacity, K_{DR} (mol^2/kJ^2) is the constant related to the mean sorption energy, ε (kJ/mol) is the Polanyi potential. R (kJ/mol K) is the ideal gas constant, T (K)is the temperature and E (kJ/mol) is the mean adsorption energy that is required to transfer 1mol of ions from liquid phase to solid surfaces.

In order to evaluate the suitability of a model equation to experimental results, an error function assessment is usually required. The best fitting equilibrium isotherm models were validated using coefficient of determination (R^2) and Chi-square (χ^2).

The non-linear optimization technique was applied for calculating the adsorption parameters from these models (Table 3). The R^2 and χ^2 values for both models indicated a good fit between the experimental and isotherm data. The maximum adsorption capacity of Langmuir (Q^0_{max}) was 72.796 mg/g, 39.889 mg/g, 28.034 mg/g and 25.096 mg/g for the B-NaOH, B-$MgCl_2$, B-H_2SO_4 and RB, respectively. Langmuir isotherm can also be interpreted to predict the affinity between copper and bentonites using constant separation factor (R_L) (dimensionless) of the solid-liquid adsorption system defined by the equation (Equation(14))[61]:

$$R_L = \frac{1}{1+C_0k_L} \qquad \ldots(14)$$

Where C_0 is the initial of Cu(II) concentration (mg/L) and k_L is the Langmuir constant.

The condition based on R_L values suggests that the adsorption process was unfavorable if $R_L>1$; linear when $R_L = 1$; favorable in the range $0 < R_L < 1$; or irreversible ($R_L = 0$).

In this study, R_L values were found to be 0.65-0.02, 0.58-0.01, 0.94-0.14 and 0.95-0.16 for B-NaOH, B-$MgCl_2$, B-H_2SO_4 and RB, respectively (they are in the range of 0 and 1), this indicates favourable adsorption of Cu (II) ions on each of the tested adsorbents.

Values of Freundlich equilibrium constants (n) reported in Table 3 are 0.238 - 0.476. According to the Freundlich theory[3], when n < 1 the adsorption isotherm becomes favorable. This allows confirming that the adsorption on each adsorbent is favourable for Cu(II) ions.

Using the Dubinin–Radushkevich model, the magnitudes of E were 3.713 kJ/mol, 1.149 kJ/mol, 0.244 kJ/mol and 0.243 kJ/mol for B-NaOH, B-$MgCl_2$, B-H_2SO_4 and RB, respectively. These values were <8 kJ/mol indicating that the sorption process may be physical in nature[62].

Related Works

The adsorption capacities of copper using raw and treated bentonites were compared with some results reported in previous studies based on the maximum adsorption capacity of the Langmuir (Q^0_{max}) model (Table 4). Therefore, activation of bentonite significantly enhanced its sorption capacity and that treated bentonites were a very suitable sorbents in water treatment for the removal of copper. In fact, according to all of these studies, the effectiveness of the treated bentonite was affected by many factors

Table 3 — Isotherm parameters for the adsorption of copper onto raw and treated bentonites.

Isotherm	Parameter	B-NaOH	B-$MgCl_2$	B-H_2SO_4	RB
Langmuir	Q^0max (mg/g)	72.796	39.889	28.034	25.096
	k_L (L/mg)	0.533	0.720	0.061	0.053
	R^2	0.999	0.973	0.991	0.992
	$\chi 2$	$3.576.10^{-29}$	8.026	0.844	0.563
Freundlich	K_F $((mg/g)/(mg/L))^n$	24.964	16.153	3.361	2.671
	n	0.320	0.238	0.457	0.476
	R^2	0.983	0.970	0.968	0.972
	$\chi 2$	17.229	8.881	2.879	1.950
Dubinin-Radushkevich	q_{DR} (mg/g)	65.833	37.45	20.989	18.017
	K_{DR} (mol^2/kJ^2)	$3.626x10^{-8}$	$3.786x10^{-7}$	$8.384x10^{-6}$	$8.427x10^{-6}$
	R^2	0.987	0.891	0.898	0.890
	$\chi 2$	13.416	32.477	9.224	7.572
	$E = \frac{1}{\sqrt{2K_{DR}}}$ (KJ/mol)	3.713	1.149	0.244	0.243

such as the initial pH value of the aqueous solutions, initial concentration of copper and dosage of the adsorbent. This could be also attributed to differences in the adsorbent properties including specific surface area and pore size as well as the interactions between copper and adsorbent surface.

Application on industrial wastewater

Assessment of the raw and treated bentonites have been performed for their possible use in the removal of Cu(II) ions from the industrial wastewater of the Cable Industry Company (ENICAB) located in Biskra, Algeria. The wastewater was used before treatment and without adding any metal reagents.

The *p*H of this wastewater was slightly acid (pH ~ 6.08). The conductivity was more than 1000 µS/cm, so this wastewater was highly mineralized. The presence of high levels of calcium (124 mg/L), magnesium (594 mg/L), chloride (784 mg/L) and sulfate (754 mg/L) were noted in this wastewater. The mean concentration of copper was 18.10 mg/L. Such concentrations of this metal was well above the Algerian standard for liquid industrial discharges (0.5 mg/L) indicated in the Official Journal of the Algerian Republic[63].

The monitoring of copper adsorption kinetics (Fig. 7) has revealed high efficiency for copper removal (Table 5). As in the case of synthetic solutions, the adsorption kinetics were well described by the PSO nonlinear model. In addition, the order of effectiveness of the tested adsorbents varied as follows:

B-NaOH> B-MgCl$_2$> B-H$_2$SO$_4$> RB.

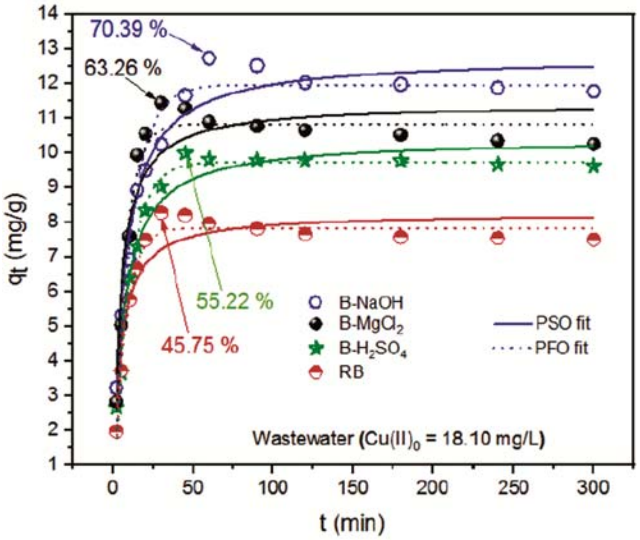

Fig. 7 — Effect of contact time on the Cu(II) adsorption onto raw and treated bentonites and plots of kinetic models (Pseudo-first-order (PFO), Pseudo-second-order (PSO)) in wastewater (Cu(II)$_0$ = 18.10 mg/L, dose of adsorbent = 1 g/L, pH$_0$ = 6.08).

Table 4 — Comparison of maximum adsorption capacities of Langmuir (Q^0_{max}) of Cu (II) on raw and treated bentonite reported in the literature.

Adsorbent	Operating conditions	Q^0_{max} of Langmuir (mg/g)	Reference
- Raw bentonite of Mastaganem NW of Algeria	Cu : 10-100 mg/L	25.096	
- Bentonite-H$_2$SO$_4$	Dose of adsorbent = 1 g/L	28.034	This study
- Bentonite-MgCl$_2$	Initial *p*H= 5.5	39.889	
- Bentonite-NaOH		72.796	
- Raw bentonite	Cu: 10-100 mg/L	12.2 mg/g	22
- Treated bentonite - 5 N H$_2$SO$_4$	Mount of clay= 0.2 g	15.4 mg/g	
	Initial *p*H = 6.5		
- Bentonite of Maghnia (NW Algeria)–CaCl$_2$	Adsorbent 100 mg in 50 mL of solution, Initial *p*H = 5.0	55.476 mg/g	26
- Acid activated bentonite of Mostagenem	Masse of clay = 1g	7.1 mg/g	20
0.05 M HCl	Shaking time= 1h	10.44 mg/g	
0.5 M HCl	T =25 °C		
- Bentonite of Thai Nippon Chemical Industry LTD		30.99	14
- Bentonite-NaOH	Cu: 5.5-100 mg/L	74.97	
- Bentonite- H$_2$SO$_4$	Dose of adsorbent = 2 g/L	52.85	
- Bentonite-HCl		56.30	
- Bentonite (Fisher Scientific)	Cu : 100-500 mg/L	248.93 mg/g	31
- Bentonite+ Graphite powder composite	Adsorbent: 50 mg in 100 mL of solution, Initial *p*H = 6	558.36 mg/g	

Table 5 — Kinetic parameters of the PFO and the PSO models for adsorption of Cu(II) ions in wastewater ($(Cu(II))_0$= 18.10 mg/L, dose of adsorbent = 1 g/L, pH_0 = 6.08).

Parameter	B-NaOH	B-$MgCl_2$	B-H_2SO_4	RB
Removal of copper (%)	70.392	63.265	55.216	45.746
Equilibrium time (min)	60	30	45	30
$q_{e, exp}$ (mg/g)	12.741	11.451	9.995	8.28
$q_{e, calc}$ PFO (mg/**g**)	11.969 $R^2 = 0.956$	10.839 $R^2 = 0.972$	9.746 $R^2 = 0.984$	7.838 $R^2 = 0.980$
$q_{e, calc}$PSO (mg/**g**)	12.783 $R^2 = 0.965$	11.425 $R^2 = 0.984$	10.407 $R^2 = 0.962$	8.271 $R^2 = 0.903$

Conclusion

Protocols were developed to obtain low cost adsorbents from naturally abundant Algerian bentonite (RB) using NaOH, H_2SO_4 and $MgCl_2$ as agents of activation. Results of raw and treated bentonites characterization have confirmed that montmorillonite, illite and kaolinite are major minerals clay identified and the detected functions proved the aluminosilicate composition of the clays. Calcium is the predominant cation in raw bentonite (RB) and its structure has changed after treatment with activation agents. Results obtained from the adsorption experiments revealed that in synthetic solutions, the highest removal efficiency of Cu(II) ions was observed for B-NaOH it exceeded 99%. Kinetic experiments indicated the best fitting to the pseudo-second-order kinetic model. From the study of the intraparticle diffusion, three steps governed the copper adsorptions onto raw and treated bentonites. And the first linear portions had the steepest slopes which suggest the rapid retention of Cu(II) ions on the exterior surfaces at the beginning of adsorption. Several possible adsorption mechanisms were elaborated which include cation exchange and interactions between Cu(II) ions and protonated aluminol and silanol groups in bentonite. In addition, the adsorption at higher *p*H values (> 7) include the formation of metal complexes ($Cu_2(OH)_2^{2+}$, $CuOH^+$ and $Cu(OH)_3^-$) and hydroxide precipitation ($Cu(OH)_2$). The efficiency of copper adsorption on these clays increased by increasing the adsorbent dosage from 0.1 to 4 g/L. In addition, it decreases with the increase of the initial copper content.The corresponding parameters of equilibrium adsorption isotherm indicated that the sorption mechanism might be physical in nature. The maximum adsorption capacities of Cu(II), based on Langmuir model were 25.1 mg/g, 28.03 mg/g, 39.89 mg/g and 72.80 mg/g for RB, B-H_2SO_4, B-$MgCl_2$ and B-NaOH respectively.

The application of removal of Cu(II) from industrial wastewater of cable industries indicated that the order of effectiveness of the adsorbents tested varies as follows: B-NaOH (70.39 %)> B-$MgCl_2$ (63.27 %)> B-H_2SO_4 (55.22 %) > RB (45.75 %).

As conclusion, the tested bentonites particularly the ones treated in the presence of NaOH (B-NaOH) can be used as potential and effective adsorbent for the removal of copper from aqueous solution. This could be attributed to the fact that it is an efficient process and that bentonite reserves are widely available in Algeria.

Acknowledgement

This study was motivated by Research Laboratory in Subterranean and Surface Hydraulics, Civil Engineering and Hydraulic Department, University of Biskra and the General direction of Scientific Research and Technological Development of the Ministry of Higher Education and Scientific Research- Algeria.

Conflict of interest

On behalf of all authors, the corresponding author states that there is no conflict of interest.

References

1 Poltelon J L & Zysman K, *Le guide des analyses de l'eau potable*, Edition, La Lettre du Cadre Territorial, Voiron, France, (1998).

2 Wang W, Hua Y, Li S, Yan W & Zhang W, *Chem Eng J*, 304 (2016) 79.

3 Amer M W & Awwad A M, *Asian J Chem*, 29 (2017) 965.

4 WHO (World Health Organization). Guidelines for drinking-water quality, incorporating the first and second addenda, third edition Volume 1. Recommendation, Geneva, (2008).

5 Youcef L & Achour S, *Elimination de polluants des eaux (Fluor, cadmium, phosphates). Application des procédés de précipitation chimique et d'adsorption*. Presses Académiques Francophones, Sarrebruck, Allemagne, (2014).

6 Chen Q, Yao Y, Li X, Lu J, Zhou J & Huang Z, *J Water Proc Eng*, 26 (2018) 289.

7 Li X, Zhang Q & Yang B, *Chemosphere*, 239 (2020)124660.

8 Meunier N, Drogui P, Montané C, Hausler R, Mercier G & Blais J F, *J Hazard Mater*, 137 (2006) 581.

9 Wang L K, HungY T & Shammas N K, *Handbook of Environmental Engineering, Physicochemical Treatment Processes*, Humana Press Inc., Totowa, New Jersey, 3 (2005).

10 Barakat M A, *Arab J Chem*, 4 (2011) 361.

11 Tchobanoglous G T, Burton F L & Stensel H D, *Wastewater Engeneering. Treatment and reuse*. 4th Edn. McGraw-Hill. New York, United States, (2003).

12 Alalwan H A, Kadhom M A & Alminshid A H, *J Water Supply Res T Aqua*,69 (2020) 99.

13 Krstić V, Urošević T & Pešovski B, *Chem Eng Sci*, 192 (2018) 273.

14 Wongkoblap A, Ngernyen Y, Budsaereechai S & Charoenbood A, *Heavy metal removal from aqueous solution by using bentonite clay and activated carbon*. In: Chemeca 2013: Challenging tomorrow, Barton, ACT: Engineers Australia, (2013) 689.

15 Toor M & Jin B, *Chem Eng J*,187 (2012) 79.

16 Alexander J A, Zaini M A A, Surajudeen A, Aliyu El-N U &Omeiza A U*, Particul Sci Technol*, 37 (2019)538.

17 Almeida A F de Neto, Vieira M G A & Silva M G C da, *Braz J ChemEng*,31 (2014) 1047.

18 Shamim A, Anwer A & Ahmad A, *Int J Adv Eng Res Dev*, 3 (2016) 392.

19 Boufatit M, Mohammed- Aziz F & Dib S, *Anyagtudomány Mater Sci*, 63 (2011) 24.

20 Mohammed-Azizi F, Dib S & Boufatit M, *Des Water Treat*, 51 (2013) 4447.

21 Cherifi-Naci H, Boughrara S & Louhab K, *ALJEST*, 1 (2015) 11.

22 Djebbar M & Djafri F, *Water Qual Res J Can*, 51 (2015) 26.

23 Ouakouak A K & Youcef L, *Larhyss J*, 27 (2016) 39.

24 Zahaf F, Marouf R, Ouadjenia F & Schott J, *Des Water Treat*, 131 (2018) 282.

25 Bouazza D, Miloudi H, Adjdir M, TayebA & Boos A, *Appl Clay Sci*, 151 (2018) 118.

26 Ouakouak A, Rihani K, Youcef L, Hamdi N & Guergazi S, *Mater Res Express*, 7 (2020) 25045.

27 Athman S, Sdiri A & Boufatit M, *Int J Environ Res*, 14(2020)1.

28 ENOF, Rapport d'analyse des bentonites de Maghnia(Hammam Boughrara) et de Mostaganem (Mzila), Laboratoire ENOF, Maghnia, Algérie, (2017).

29 Hussain S, Ullah Z, Gul S, Khattak R, Kazmi N, Rehman F, Khan S, Ahmad K, Imad M & Khan A, *Pol J Environ Stud*, 25 (2016) 1947.

30 Sepulveda L A & Santana C C, *Environ Technol*, 34 (2013) 967.

31 Chang Y S, Iu A P, Mubarak N M, Khalid M, Jagadish, P, Walvekar R & Abdullah E C*, Environ Sci Pollutt Res*, 27 (2020) 33270.

32 Rodier J, Legube B, Merlet N & Brunet R, *L'analyse de l'eau. 9ème édition*, Dunod, Paris, France, (2009).

33 Bouazza D, Miloudi H, Sassi M, Boos A, Goetz G, Tayeb A & Bengueddach A, *J Phys Chem Solids*, 67 (2006) 1032.

34 Petit S, Decarreau A & Righi D, *Géos C R*, 33 (2003) 737.

35 Pushpaletha P, Rugmini S & Lalithambika M, *Appl Clay Sci,* 30 (2005) 141.

36 Tyagi B, Chudasama C D & Jasra R V, *Spectrochim Acta A: Mol Biomol Spectrosc*, 64 (2006) 273.

37 Liu Z, Zhao Y, Colin C, Siringan F P & WU Q, *Appl Geo Chem*, 24 (2009) 2195.

38 Baziz M, *Synthesis and Characterization of Nanocomposite polyaniline-sepiolite,* Magister memory. University of Oran, Algeria, in French, (2010).

39 Angar Y, Djelali N E & Kebbouche Gana S, *Environ Sci Pollut Res*, 24 (2016) 11078.

40 Dib S & Boufatit M, *Des Water Treat*, 5 (2009) 106.

41 Khalil A A, Abo O, El-Wafa S, Sallam A & El Korashy S A, *Mag Verfahrenstech*, 12 (1988) 396.

42 Lagergren S, *K Sven VetenskHandl*, 24 (1898) 1.

43 Blanchard G, Maunaye M & Martin G, *Water Res*, 18 (1984) 1501.

44 McLintock I, *Nature*, 216 (1967) 1204.

45 Weber W J & Morris J C, *J Sanit Eng Div Am Soc Civil Eng*, 89 (1963) 31.

46 Hossain M A, Ngo H H, Guo W S & Nguyen T V, *Bioresour Technol*, 113 (2012) 97.

47 Ho Y S & Ofamaja A E, *J Hazard Mater,* 129 (2006) 137.

48 Boparai H K, Joseph M & O'Carroll D M, *J Hazard Mater*, 186 (2011) 458.

49 XuW,Chen Y, Zhang W & Li B, *Adv Powder Technol*, 30 (2019) 493.

50 Putra E K, Pranowo R, Sunarso J, Indraswati N & Ismadji S, *Water Res*, 43 (2009) 2419.

51 Chai J B, Au P I, Mubarak N M, Khalid M, Ng W P Q, Jagadish P, Walvekar R & Abdullah E C, *Environ SciPollut Res Int*, 27 (2020) 13949.

52 Dai Y, Zhang K, Li J, Jiang Y, Chen Y & Tanaka S, *Sep Purif Technol*,186 (2017) 255.

53 Allison J D, Brown D S & Novo Gradac K J, *MINTEQA2/PRODEFA2, a geochemical assessment model for environmental systems: version 3.0 user's manual 1991*, Environmental Research Laboratory, Office of Research and Development, US, (1991).

54 Gustafsson J P, *Visual MINTEQ 3.0 user guide.* KTH (Department of Land and Water Recources, Stockholm, Sweden), (2011).

55 Ding S, Sun Y, Yang C & Xu B, *Mining Sci Technol, China*, 19 (2009) 489.

56 Liu H, Xie S, Liao J, Yan T, Liu Y & Tang X, *J Radioanal Nucl Chem*, 317 (2018) 1349.

57 Yang S, Zhao D, Zhang H, Lu S, Chen L & Yu X, *J Hazard Mater*, 183 (2010) 632.

58 Langmuir I, *J Am Chem Soc*, 40 (1918) 1361.

59 Freundlich H M F, *Uber die adsorption in losungen. Zeitschrift fur Physikalische Chemie*, Leipzig, 57A, (1906) 385.

60 Dubinin M & Radushkevich L, *Proc Acad Sci Phys Chem Sect USS*, 55 (1947) 331.

61 Vunain E, Kenneth D & Biswick T, *Appl Water Sci*, 7 (2017) 4301.

62 Almohammadi S & Mirzaei M, *A E T,* 2 (2016) 85.

63 OJAR, Executive Order No. 06-141 of 19 April 2006 , section 1, article 3, *Official Journal of the Algerian Republic*, (2006).